BIOCHEMISTRY
including biophysical chemistry & molecular biology
Article

*Biochemistry* **2011,** *50,* 1771–1777 1771
DOI: 10.1021/bi101912q

# Coordination Features and Affinity of the $Cu^{2+}$ Site in the α-Synuclein Protein of Parkinson's Disease[†]

Christopher G. Dudzik,[‡] Eric D. Walter,[§] and Glenn L. Millhauser*[,‡]

[‡]*Department of Chemistry and Biochemistry, University of California, Santa Cruz, California 95064, United States, and* [§]*Pacific Northwest National Laboratory, P.O. Box 999, K8-98, Richland, Washington 99352, United States*

*Received November 30, 2010; Revised Manuscript Received January 24, 2011*

ABSTRACT: Parkinson's disease (PD) is the second most prevalent age-related, neurodegenerative disorder, affecting >1% of the population over the age of 60. PD pathology is marked by intracellular inclusions composed primarily of the protein α-synuclein (α-syn). These inclusions also contain copper, and the interaction of $Cu^{2+}$ with α-syn may play an important role in PD fibrillogenesis. Here we report the stoichiometry, affinity, and coordination structure of the $Cu^{2+}$−α-syn complex. Electron paramagnetic resonance (EPR) titrations show that monomeric α-syn binds 1.0 equiv of $Cu^{2+}$ at the protein N-terminus. Next, an EPR competition technique demonstrates that α-syn binds $Cu^{2+}$ with a $K_d$ of ≈0.10 nM. Finally, EPR and electron spin echo modulation (ESEEM) applied to a suite of mutant and truncated α-syn constructs reveal a coordination sphere arising from the N-terminal amine, the Asp2 amide backbone and side chain carboxyl group, and the His50 imidazole. The high binding affinity identified here, in accord with previous measurements, suggests that copper uptake and sequestration may be a part of α-syn's natural function, perhaps modulating copper's redox properties. The findings further suggest that the long-range interaction between the N-terminus and His50 may have a weakening effect on the interaction of α-syn with lipid membranes, thereby mobilizing monomeric α-syn and hastening fibrillogenesis.

Parkinson's disease (PD)[1] is the second most prevalent neurological disorder after Alzheimer's disease, affecting >1% of the U.S. population over the age of 60 (*1*). PD, an idiopathic neuropathy, is chronic, progressive, and often fatal. Clinical symptoms of PD include diminished motor function, tremors, and speech disorders, attributed to the progressive loss of dopaminergic neurons of the *substantia nigra* (*2*). Hallmarks of affected dopaminergic neurons are Lewy bodies, cytosolic filamentous inclusions composed primarily of the protein α-synuclein (α-syn). The correlation between α-syn and PD has been clearly demonstrated in animal models where α-syn overexpression leads to PD-like motor deficits and intracellular deposits reminiscent of Lewy bodies (reviewed in ref *3*). Furthermore, hereditary early onset PD in humans is linked to genetic mutations in α-syn or copy number variation (*4*, *5*).

α-Synuclein is a 140-residue, intrinsically disordered protein that is localized primarily to the presynaptic termini of dopaminergic neurons (Figure 1) (*6*). The segment termed the non-A$\beta$ component (NAC), residues 61−95, is dominated by hydrophobic residues and tends to form aggregates leading to the parallel $\beta$-sheet rich fibril structures present in LB (*7*, *8*). Aggregates from the NAC also contribute approximately 10% of the protein in the senile plaques in Alzheimer's disease patients (*9*). The N-terminal region of α-syn, encompassing the NAC (residues 9−97), possesses a series of 11-residue imperfect repeats that form an amphipathic α-helix when associated with lipid vesicles, a structure similar to exchangeable apolipoproteins (*10*, *11*). The C-terminal tail is highly acidic and devoid of secondary structure. However, truncation of this segment produces a shortened lag time in fibril kinetics studies, suggesting a possible autoinhibitory role protecting against α-syn polymerization (*12*).

While the primary cause of α-syn aggregation in PD is unknown, there is a growing body of evidence implicating environmental factors such as long-term exposure to heavy metals (*13*−*16*). The *substantia nigra* region of PD-affected brains has been shown to have an increase in iron content (*17*), and $Cu^{2+}$ levels are significantly increased in the cerebrospinal fluid (CSF) of PD patients (*18*). It is well-documented that α-syn interacts with $Cu^{2+}$, a prevalent species of the CSF, leading to enhanced aggregation and in vitro polymerization (*19*−*22*).

The interaction between α-syn and $Cu^{2+}$ may also play a role in the protein's normal physiological function. Other neurodegenerative proteins, such as A$\beta$ in Alzheimer's disease and PrP in the prion diseases, take up copper (*23*−*25*). Unambiguous functions have not yet been identified in these cases, but the regulation of copper homeostasis and redox activity are common themes. Most α-syn is intracellular, where copper is found predominantly in the $Cu^{+}$ state, but a fraction is secreted to the oxidizing extracellular space that favors $Cu^{2+}$ (*26*). Synaptic $Cu^{2+}$ concentrations range from 2 to 200 $\mu$M (*27*), well in excess of the affinities of α-syn for $Cu^{2+}$ measured by most laboratories. Moreover, the *substantia nigra* is part of the *basal ganglia*, which exhibits among the highest copper concentrations of the CNS (*21*, *28*). Perhaps α-syn is another player in the line of defense against uncomplexed copper, with action localized to the membrane surface. Moreover, $Cu^{2+}$ facilitates oxidation of the

[†]This work was supported by National Institutes of Health Grant GM065790.

*To whom correspondence should be addressed. Phone: (831) 459-2176. Fax: (831) 459-2935. E-mail: glennm@ucsc.edu.

[1]Abbreviations: α-syn, human α-synuclein; CNS, central nervous system; CSF, cerebrospinal fluid; DLS, dynamic light scattering; EPR, electron paramagnetic resonance; ESEEM, electron spin echo envelope modulation; $K_d$, dissociation constant; LB, Lewy bodies; NAC, non-A$\beta$ component; PD, Parkinson's disease.


Published on Web 01/25/2011

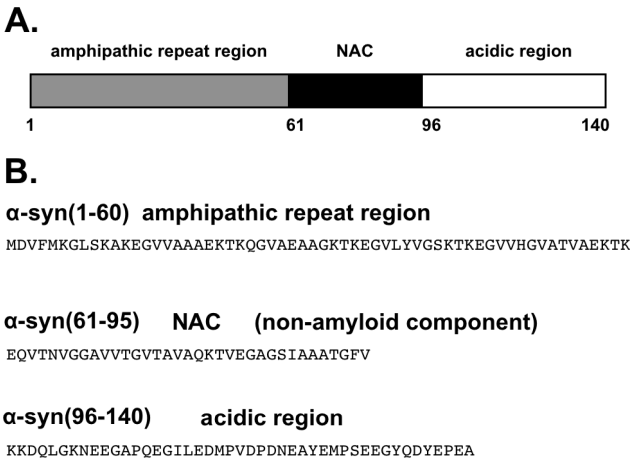


FIGURE 1: Features of the α-synuclein primary structure identifying (A) the three consensus segments and (B) the amino acid sequence associated with each segment. Residues 9−97, encompassing the amphipathic repeat region and the NAC, form an extended helix when associated with lipid membranes.

N-terminal methionine in α-syn, which hinders in vitro fibril formation (*29*).

Despite the need to clearly characterize the interaction between α-syn and $Cu^{2+}$, there is still uncertainty regarding the α-syn-$Cu^{2+}$ binding stoichiometry, affinity, and coordination structure (reviewed in ref *30*). Potentiometric studies performed on α-syn-derived N-terminal peptides suggest that $Cu^{2+}$ is coordinated by nitrogens from the N-terminal amine, the Asp2 backbone nitrogen amide, and the His50 imidazole, and an oxygen from the Asp2 carboxylic acid (*31*, *32*). These findings are consistent with Trp fluorescence quenching experiments, which also show a preference for copper binding to the N-terminal region (*33*). Electron paramagnetic resonance (EPR) on full-length (140-residue) α-syn suggests a coexistence of structures involving the N-terminus and His50, and that His50 participation may be facile (*34*). NMR line intensity measurements contrast this and suggest instead that there are no long-range coordination structures, but rather a series of local $Cu^{2+}$ sites distributed about the N-terminus, His50, and several areas of negatively charged residues in the C-terminal tail (*35*).

Reported affinity measurements also yield variation. Circular dichroism titrations identify two $Cu^{2+}$ sites with dissociation constants of 0.7 and 60 $\mu$M (*36*). Fluorescence quenching probed by a Trp at position 4 identifies tighter interaction, with a dissociation constant of 100 nM (*37*). Finally, isothermal titration calorimetry (ITC) of exchange with a soluble copper−glycine complex finds a single $Cu^{2+}$ site in wild-type α-syn, with a dissociation constant of approximately 0.2 nM (*38*).

While most of the studies described above point to the involvement of the α-syn N-terminal domain in $Cu^{2+}$ uptake, the role of other protein segments, most notably His50, remains unclear, and as noted above, reported affinity measurements vary by approximately 3 orders of magnitude. Here we apply continuous wave (cw) and pulsed EPR to the wild type and a panel of mutant α-syn species, at varying stoichiometric ratios. There are three elements to this study. First, through titration studies, we examine the number of $Cu^{2+}$ binding sites and, more generally, how the protein responds to increasing levels of the metal ion. Next, using mutagenesis, we identify the residues responsible for the primary binding sites. Finally, competition studies are applied to evaluate affinity. While our studies support the involvement of the α-syn N-terminal domain, we find strong evidence of the participation of His50, especially at a 1:1 copper:protein ratio. Moreover, we find that the affinity at this ratio is very high, with a $K_d$ value consistent with the lowest reported value in the current literature, thus pointing to a physiological role for the α-syn−$Cu^{2+}$ interaction.

## MATERIALS AND METHODS

*Proteins and Reagents*. The human wild-type α-syn gene cloned into the *pRK172*/α-*synuclein* plasmid vector was a generous gift from the Fink lab at the University of California (Santa Cruz, CA). The primers for the H50A and Q98Stop mutations were obtained from Invitrogen. Mutations were performed using the GeneTailor Site Directed Mutagenesis System (Invitrogen catalog nos. 12397-014 and 12397-022). α-syn, α-syn(1−97), and α-syn(H50A) were recombinantly expressed in *Escherichia coli* BL21(DE3) competent cells (Invitrogen, Carlsbad, CA) using an autoinduction procedure of Kim et al. described previously (*39*). Cells were harvested by centrifugation followed by sonication in lysis buffer [50 mM NaCl, 20 mM Tris, 0.2 mM PMSF (phenylmethanesulfonyl fluoride), 10% (v/v) Triton X-100 (Sigma) (pH 7.4)]. Purification was performed using two rounds of ammonium sulfate precipitation (first round at 0.164 g/mL, second round at 0.117 g/mL) followed by centrifugation, resuspension in 6 M guanidine HCl, and reverse-phase HPLC (C4 column on a Thermo Scientific instrument). All peptides were synthesized using fluorenylmethoxycarbonyl (Fmoc) methods as described previously (*40*).

*Electron Paramagnetic Resonance*. Samples were prepared in degassed buffer containing 25 mM MOPS buffer and 25% (v/v) glycerol, where the glycerol served as a cryoprotectant. All cw X-band spectra ($\nu$ = 9.44 GHz, microwave power in the range of 0.6−5.0 mW, modulation amplitude of 5.0 G, and sweep width of 1200 G) were recorded at approximately 125 K, using a Bruker EleXsys spectrometer and an SHQ (Bruker) cavity equipped with a variable-temperature controller. Competition assays were performed as described in the text, and resultant composite spectra were analyzed using non-negative least-squares (NNLS) in the Matlab program suite. Three-pulse ESEEM measurements were obtained at 20 K on a Bruker E580 X-band spectrometer using a dielectric resonator and an Oxford CF 935 cryostat. A $\pi/2-\tau-\pi-T-\pi/2-\tau-$echo sequence with pulse lengths of 12, 24, and 12 was used. The initial value of $\tau$ was 136 ns, and $T$ was lengthened in 799 steps of 12 ns each with 100 samples per step.

*Dynamic Light Scattering*. Hydrodynamic dimensions were estimated using dynamic light scattering on a DynaPro Molecular Sizing Instrument (Protein Solutions, Lakewood, NJ) using a 1.5 mm path length 12 $\mu$L quartz cuvette. All experiments were conducted at 35 $\mu$M protein in 75 mM MOPS/NEM buffer (pH 7.4) after centrifugation for 20 min at 13000 rpm

## RESULTS

*Stoichiometry*. The copper:α-syn binding stoichiometry was determined by EPR titration at pH 7.4 and referenced against a calibrated copper-EDTA standard. Specifically, $Cu^{2+}$ (delivered as copper acetate) was titrated to a fixed concentration of protein. The integrated cw EPR spectrum (double integral of the first-derivative EPR signal) is directly proportional to the amount of bound $Cu^{2+}$. Normalized copper spectra at 1, 2, and 4 equiv (Figure 2) are characteristic of a type 2 (oxygen and nitrogen)

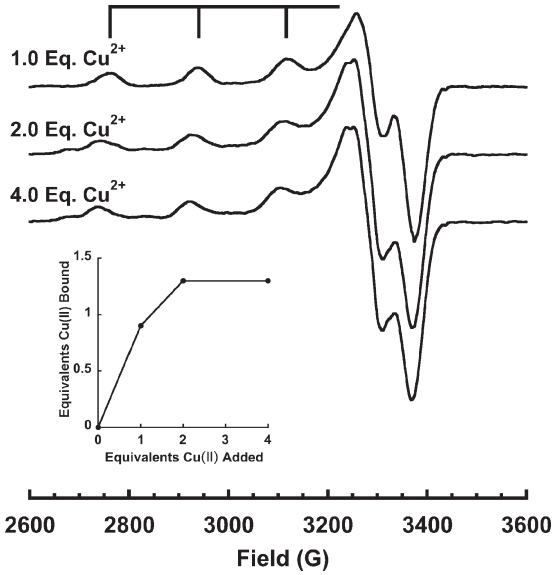


FIGURE 2: X-Band EPR spectra of α-syn at pH 7.4 with 1, 2, and 4 equiv of $Cu^{2+}$. Specra were recorded at 111 K, $\nu = 9.44$ GHz, with a sweep width of 1200 G. The inset shows EPR-detected $Cu^{2+}$ as a function of added $Cu^{2+}$ concentration and demonstrates saturation at approximately 2.0 equiv. However, competition studies find that the second equivalent is weakly coordinated.

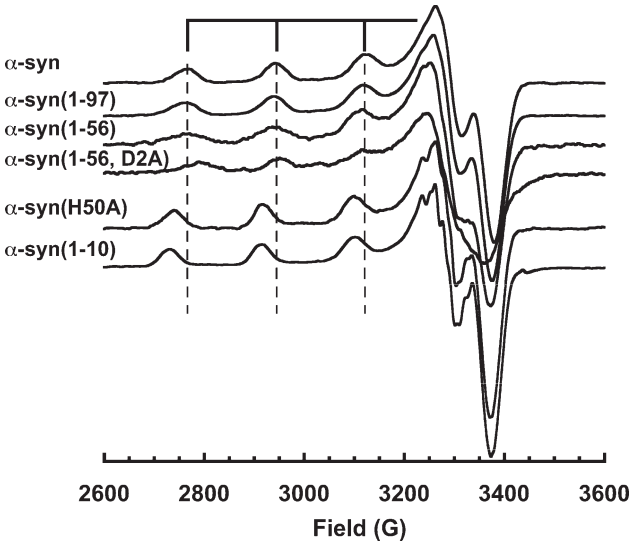


FIGURE 3: X-Band EPR spectra of α-syn, mutants, and truncated species. Vertical lines correspond to the parallel hyperfine features of wild-type α-syn. α-syn(1−97) gives a spectrum that superimposes on that of the wild type, but all other species exhibit significant variation. α-syn(1−10) and α-syn(H50A) give equivalent spectra, but they are distinct from that of the wild type, demonstrating the involvement of His50 in the coordination sphere.

coordination environment, with well-resolved splittings between the parallel hyperfine lines. At 1 equiv of $Cu^{2+}$, the EPR spectrum gives a single set of hyperfine lines, whereas at ≥2 equiv, there is a shift toward a lower field, along with the emergence of an additional overlapping spectrum. The implications of these spectra are discussed further below. Spectral integration versus added $Cu^{2+}$, shown in the inset, demonstrates that copper uptake reaches a maximum with addition of 2 equiv. Consistent with saturation of α-syn at 2 equiv of copper, we observe no change in spectral details between 2 and 4 equiv.

Although α-syn saturates at a 2:1 copper:protein ratio, the integrated spectra reveal only 1.3 bound equivalents (vertical axis of the inset in Figure 2). This is in contrast to our previous work with the octarepeat domain of the prion protein, for example, where each added equivalent is directly reflected in the integrated EPR signal. We considered several possible mechanisms that would lead to a lower than expected signal integral. First, with two bound $Cu^{2+}$ ions, there could be diamagnetic coupling between the sites, giving rise to a singlet ground state. This is observed in multinuclear copper complexes and in proteins that have bridging imidazoles between $Cu^{2+}$ centers. The coexistence of singlet and triplet states gives rise to a strong non-Curie temperature dependence. We examined the integral of α-syn upon addition of 2 equiv of copper from 20 to 120 K (data not shown) and found typical $1/T$ dependence, which likely rules out coupled copper centers.

Next, we considered whether α-syn, in the presence of copper, formed dimers or well-defined oligomers. For example, an α-syn dimer that saturates at 3 equiv of copper would give a maximal copper:protein ratio of 1.5, approximately what is observed in the titration of Figure 2. We used dynamic light scattering (DLS) to assess the protein hydrodynamic radius ($R_H$) and thus whether α-syn remains monomeric in the presence of copper. Experiments were performed with α-syn in buffer, and with 1 or 2 equiv of $Cu^{2+}$ (data not shown). In all cases, a single peak corresponding to a hydrodynamic radius of 3.3 ± 0.2 nm dominated, with no evidence of dimers, trimers, or other well-defined oligomers. Moreover, the measured hydrodynamic radius is consistent with the expected value for a 140-amino acid random coil polypeptide (*41*).

Finally, we considered whether the second added equivalent is weakly bound and in equilibrium with aquo copper [as EPR silent $Cu(OH)_2$ complexes]. To address this possibility, we used the prion-derived peptide HGGGW as a competitor. This well-characterized species binds $Cu^{2+}$ with a dissociation constant of 7.0 μM. Addition of 1.0 equiv of HGGGW to a 1.5:1 $Cu^{2+}$/α-syn mixture completely eliminated the α-syn EPR spectrum associated with the second $Cu^{2+}$ equivalent. In its place, we observed the characteristic spectrum of the $Cu^{2+}$−HGGGW complex, and within experimental error, spectral integration accounted for 1.5 equiv of $Cu^{2+}$. Consequently, the peptide HGGGW efficiently competes away the second $Cu^{2+}$ equivalent from α-syn, demonstrating a low-affinity interaction characterized by a $K_d$ of ≫7 μM. We conclude from these experiments that while α-syn takes up 2 equiv of $Cu^{2+}$, the second equivalent binds with low affinity and is not physiologically important. These results are in good agreement with recent findings of Hong and Simon, who used isothermal titration calorimetry to identify a single high-affinity copper site in α-syn (*38*).

*Identification of the $Cu^{2+}$ Coordination Features*. To determine the smallest segment of wt α-syn that possesses all the functional groups that directly coordinate $Cu^{2+}$, we developed a panel of truncated and chemically modified α-syn variants. These include α-syn(1−10), α-syn(1−56), α-syn(1−97), and several N-terminally acetylated species. At 1 equiv of $Cu^{2+}$, α-syn(1−56) and α-syn(1−97) give spectra that nearly overlap with that of the wild type (Figure 3). However, upon addition of a second $Cu^{2+}$ equivalent, only α-syn(1−97) shows a shift in the parallel region similar to that observed in full-length α-syn. In contrast, while α-syn(1−10) takes up 1 equiv of $Cu^{2+}$, the bound species gives an EPR spectrum that does not overlap with that of a 1:1 $Cu^{2+}$/α-syn(1−97) mixture or a 1:1 full-length mixture. Acetylation of any of the α-syn variants completely abrogates copper uptake (data not shown). Together, these data demonstrate that the

Table 1: EPR Parameters

| protein | $g_{\|\|}$ | $A_{\|\|}$ (G) |
|---|---|---|
| α-synuclein | 2.226 | 178.6 |
| α-syn(1−10) | 2.245 | 183.3 |
| α-syn(1−56) | 2.229 | 173.2 |
| α-syn(1−97) | 2.226 | 178.6 |
| α-syn(H50A) | 2.242 | 176.6 |

α-syn N-terminus participates in $Cu^{2+}$ coordination (*42*), but residues beyond the first 10 are required to recapitulate the coordination environment of wild-type α-syn.

To identify the specific residues required for copper coordination, we introduced point mutations into both synthetically produced peptides and recombinantly expressed α-syn protein. $A_{||}$ and $g_{||}$ values derived from the EPR spectra (shown in Table 1) are consistent with a 3N1O coordination environment, as determined from Peisach−Blumberg correlations. In addition, previous potentiometric studies suggest that Asp2 is involved in Cu(II) binding (*31*, *32*). Indeed, peptide coordination of metal centers with the second aspartate residue following a free peptide N-terminus gives very stable $Cu^{2+}$ complexes (*43*). To directly test for this, we prepared α-syn(1−56) with a D2A point mutation. EPR spectra of 1:1 $Cu^{2+}$ complexes with α-syn(1−56) and α-syn(1−56,D2A) reveal differences in the intense perpendicular features at approximately 3300 G and in the parallel hyperfine splittings, in turn suggesting a direct interaction with the aspartate side chain.

Next we considered His50. Although distal from the N-terminus of α-syn, imidazole is an avid copper binding group, and experiments described above suggest participation from residues beyond the first 10. EPR spectra of wild-type α-syn and α-syn(H50A), each with 1 equiv of $Cu^{2+}$, were compared as shown in Figure 3. The parallel region for the mutant species exhibits great splitting (larger $A_{||}$) consistent with replacement of an equatorial nitrogen with an oxygen. Moreover, this spectrum does not overlap with that of the wild type with either 1.0 or 2.0 equiv of $Cu^{2+}$.

To further assess the involvement of H50 in $Cu^{2+}$ coordination, we used electron spin echo envelope modulation (ESEEM). ESEEM is a pulsed EPR technique with sensitivity to spin-active nuclei approximately 10 Å from the paramagnetic copper center (*44*). At X-band frequencies, the distal $^{14}N$ ($I = 1$) of a coordinated imidazole ring gives characteristic quadrupolar transitions and is diagnostic for interacting His side chains (*45*). The FT ESEEM of α-syn with 1.0 equiv of $Cu^{2+}$ shown in Figure 4 is typical for imidazole, with three low-frequency peaks that correspond to transitions among $^{14}N$ quadropolar levels in exact cancellation, as well as the ≈4 MHz peak from the noncancelled electron spin manifold. We also find that α-syn(H50A) fails to give an ESEEM spectrum with 1.0 equiv of $Cu^{2+}$. Together, these findings demonstrate unequivocally the equatorial coordination by the H50 imidazole (*40*). The spectra in Figure 4 further show that the H50 coordinates $Cu^{2+}$ in wild-type α-syn and in truncated α-syn(1−97) even in the presence of excess metal ion. Addition of 2.0 equiv of $Cu^{2+}$, however, brings out additional low-intensity peaks at approximately 2 and 2.8 MHz. Past work from our lab on the octarepeat domain of the prion protein demonstrated that these lines can arise from the $^{14}N$ of an amide group coordinated through the carboxyl oxygen, as shown in the spectrum for the $Cu^{2+}$−HGGGW complex (*40*). The appearance of these transitions in α-syn suggests that the weakly bound second $Cu^{2+}$ equivalent coordinates in a similar fashion.

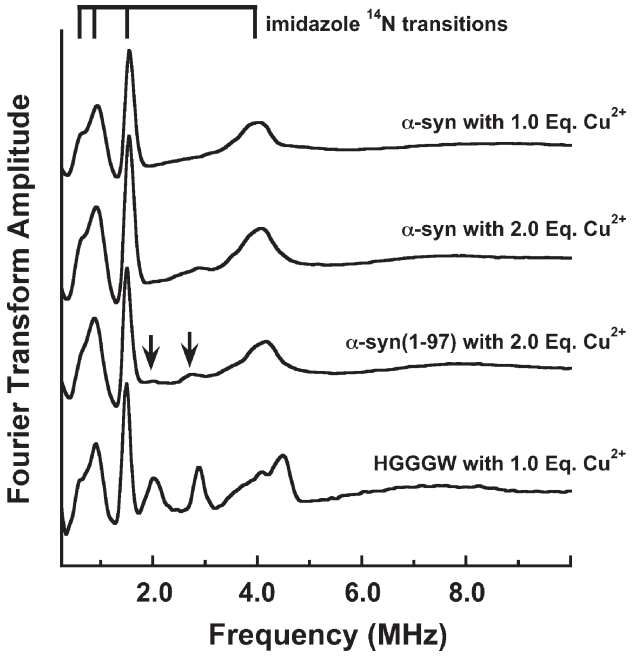


FIGURE 4: Three-pulse ESEEM spectra of α-syn with 1.0 and 2.0 equiv of $Cu^{2+}$, α-syn(1−97) with 2.0 equiv of $Cu^{2+}$, and prion protein sequence HGGGW with 1.0 equiv of $Cu^{2+}$. These spectra reveal the expected quadrupolar transitions associated with an imidazole remote nitrogen and demonstrate coordination by His50. α-syn(H50A) fails to give an ESEEM spectrum. α-syn(1−97) with 2.0 equiv of $Cu^{2+}$ gives additional weak features at 2.0 and 2.8 MHz (arrows), similar to peaks observed for the HGGGW peptide and assigned to an amide nitrogen coordinated through the backbone carbonyl.

Additional tests were performed to evaluate whether the H50 segment alone of α-syn is capable of taking up $Cu^{2+}$ with high affinity. We prepared an acetylated 21-residue peptide corresponding to a segment of α-syn with H50 in the center [α-syn(39−60)]. Titration up to 1.0 equiv of $Cu^{2+}$ gave a very weak EPR spectrum (reflecting < 10% of added copper) inconsistent with a bound species.

*Binding Affinity*. To evaluate the dissociation constant, $K_d$, of the $Cu^{2+}$−α-syn complex, we used an EPR competition technique previously developed in our lab (*46*). High-affinity competitors that take up $Cu^{2+}$ with a 1:1 stoichiometry are added to a $Cu^{2+}$/α-syn solution. Both oxidized glutathione and pentaglycine peptides are well-characterized chelators and give $Cu^{2+}$ EPR spectra that are distinct from that of the $Cu^{2+}$−α-syn complex. Spectral decomposition gives the ratio of copper bound to α-syn and specific competitor. Analysis using the known $K_d$ of the competitor determines the α-syn dissociation constant. With this approach, the amount of competitor may be varied to ensure that both bound species give resolvable EPR spectra with similar signal strengths. Table 2 shows that wt α-syn binds 1 equiv of $Cu^{2+}$ with a $K_d$ of either 0.11 or 0.15 nM, as determined from independent experiments with pentaglycine or oxidized glutathione, respectively. These values are approximately 5 orders of magnitude lower than the $K_d$ of $> 7\ \mu M$ found for the second equivalent, as described above. Consequently, these data further support the finding that α-syn takes up only 1 equiv of $Cu^{2+}$ with high affinity. To test for H50 coordination, we also performed competition experiments on the α-syn H50A mutant. As determined from both competitors, this species exhibits an approximately 4-fold lower affinity than the wild type.

Table 2: Dissociation Constants (nanomolar) Determined from Competition Studies

| protein | pentaglycine ($K_d$ = 40 nM) | oxidized glutathione[a] ($K_d$ = 0.066 nM) |
|---|---|---|
| α-synuclein | 0.11 ± 0.03 | 0.15 |
| α-syn(H50A) | 0.40 ± 0.01 | 0.60 |

[a] $K_d$ determinations using oxidized glutathione were performed once and do not have standard errors.

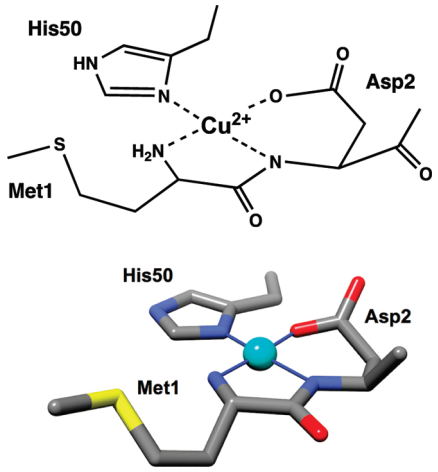


FIGURE 5: Coordination features of the primary $Cu^{2+}$ site in α-syn identified here in bond line (top) and stick (bottom) models. Competition studies show that this complex exhibits a dissociation constant of approximately 0.1 nM.

## DISCUSSION

Our EPR experiments demonstrate that the $Cu^{2+}$ coordination environment in α-syn involves the N-terminal amine and the carboxylate side chain of Asp2. In addition, ESEEM reveals participation by the H50 imidazole. To account for 3N1O coordination, suggested by evaluation of the magnetic tensor values, we propose the involvement of the Asp2 backbone amide nitrogen. Further supporting this assignment, the lack of amide $^{14}N$ couplings in the ESEEM spectra rules against Met1 backbone carbonyl coordination (*40*). Our findings at pH 7.4 suggest a well-defined coordination environment without evidence of structural heterogeneity. The coordination features are shown in Figure 5. The involvement of the N-terminal residues is consistent with studies from peptide-based $Cu^{2+}$ coordination complexes with an Asp as the second amino acid (*43*), and while α-syn may take up a second $Cu^{2+}$ equivalent, the interaction is low-affinity and likely unimportant to physiological function. In addition, we find that the dissociation constant for the first equivalent is approximately 0.10 nM.

Certain aspects of our findings support previously published work. For example, potentiometric measurements performed with α-syn segments suggest a similar coordination environment, marked by a pH sensitivity expected for N-terminal and backbone nitrogens, and a carboxylate group (*31*, *32*). Site specific tryptophan fluorescence studies identify a 1:1 α-syn−$Cu^{2+}$ complex with the N-terminal segment as the primary anchor point (*33*). Electrospray mass spectrometry also finds a single N-terminal site (*47*), wheras MALDI finds evidence of two $Cu^{2+}$ binding sites with significantly different affinities, the tighter of which (submicromolar) is located at the N-terminus (*36*). Previous EPR experiments at pH 5.0 and 7.4 were interpreted to suggest a coexistence of two coordination spheres at the higher pH, distinguished by the involvement of His50 (*34*). While our findings certainly agree with the His-bound species, we do not find evidence of a second pH 7.4 coordination mode. The 4-fold enhanced affinity we find for wild-type α-syn versus the α-syn(H50A) mutant further supports imidazole coordination, and we do not find features of the α-syn(1−10) or α-syn(H50A) EPR spectra superimposed on that of the wild type.

Despite the emerging consensus about the molecular details of the $Cu^{2+}$ coordination sphere, there remains wide disagreement with regard to affinity. As noted in the introductory section, published values for the dissociation constant range from micromolar to nanomolar. Recently, Hong and Simon used a refined ITC approach whereby $Cu^{2+}$ is added as a glycine complex (*38*). With appropriate treatment of the complex equilibria, they determine an association constant based on heat release through a copper titration. Wild-type α-syn at pH 7.4 gives an association constant of $4.7 \times 10^9$ $M^{-1}$, corresponding to a $K_d$ of 0.21 nM. Moreover, they find no evidence of a second $Cu^{2+}$ coordination site. These results are in remarkable agreement with ours described here and support a very high affinity, mononuclear site with principal anchor points at the protein N-terminus.

The emerging biophysical evidence strongly suggests that α-syn interacts with $Cu^{2+}$ in vivo. The residues involved in copper chelation are conserved, and the protein is abundant within the cell and localized to membrane surfaces at the synaptic cleft where CSF $Cu^{2+}$ levels exceed micromolar concentrations (*26*, *48*, *49*). The subnanomolar α-syn−$Cu^{2+}$ complex $K_d$, along with the abundance of synaptic α-syn, suggests that any $Cu^{2+}$ localized to the extracellular membrane would be tightly complexed. Recent evidence suggests that copper bound to α-syn within neurons of the *substantia nigra* is stabilized in the +2 oxidation state (*50*). An intriguing possibility then is that perhaps α-syn sequesters $Cu^{2+}$ at the membrane and modulates copper's inherent redox activity. Electrochemical experiments demonstrate that the $Cu^{2+}$−α-syn complex undergoes redox cycling but favors the production of hydrogen peroxide, which is less damaging to cells than radical species often produced by weakly complexed copper (*47*).

The interaction of intracellular α-syn with synaptic vesicles is well-documented, and new evidence shows that wt α-syn interacts with SNARE complexes, perhaps as a chaperone, participating in membrane fusion (*51*−*53*). Although membrane-associated α-syn is largely helical, an extended α-helix structure is incompatible with the polypeptide wrapping back to coordinate $Cu^{2+}$ with the N-terminus and His50. We propose, therefore, that $Cu^{2+}$ provides a mechanism for the release of α-syn from the synaptic vesicle membrane, upon exposure to the extracellular environment, switching from the membrane-induced helical structure to the $Cu^{2+}$-bound structure shown in Figure 5. This same mechanism may also operate in PD. A copper-mediated weakening of the interaction between α-syn and cellular membranes could increase the soluble protein fraction, thus hastening fibrillogenesis.

In summary, α-syn interacts strongly with $Cu^{2+}$ in vitro. Whether this interaction is part of the protein's natural function,

a component in the disease process, or both is a subject for further study. Our results show that monomeric α-syn binds 1 equiv of $Cu^{2+}$ with an affinity of ≈0.1 nM. This binding mode creates a protein conformational change bringing the N-terminus and H50 into the proximity of each other. Any additional association of $Cu^{2+}$ with the protein is weak, nonspecific, and not physiologically relevant. Future work will focus on determining the role of this interaction in α-syn cycling at the cell surface, and the consequences for PD pathogenesis.

## ACKNOWLEDGMENT

We are very grateful to Drs. Stefen Stoll and David Britt (University of California, Davis, CA) for their valuable consultation on the collection and processing of the ESEEM spectra.

## REFERENCES

1. Lees, A. J., Hardy, J., and Revesz, T. (2009) Parkinson's disease. *Lancet 373*, 2055–2066.
2. Jankovic, J. (2008) Parkinson's disease: Clinical features and diagnosis. *J. Neurol., Neurosurg. Psychiatry 79*, 368–376.
3. Dawson, T. M., Ko, H. S., and Dawson, V. L. (2010) Genetic animal models of Parkinson's disease. *Neuron 66*, 646–661.
4. Chartier-Harlin, M. C., Kachergus, J., Roumier, C., Mouroux, V., Douay, X., Lincoln, S., Levecque, C., Larvor, L., Andrieux, J., Hulihan, M., Waucquier, N., Defebvre, L., Amouyel, P., Farrer, M., and Destee, A. (2004) α-Synuclein locus duplication as a cause of familial Parkinson's disease. *Lancet 364*, 1167–1169.
5. Vila, M., and Przedborski, S. (2004) Genetic clues to the pathogenesis of Parkinson's disease. *Nat. Med. 10* (Suppl.), S58–S62.
6. Yang, M. L., Hasadsri, L., Woods, W. S., and George, J. M. (2010) Dynamic transport and localization of α-synuclein in primary hippocampal neurons. *Mol. Neurodegener. 5*, 9.
7. Chen, M., Margittai, M., Chen, J., and Langen, R. (2007) Investigation of α-synuclein fibril structure by site-directed spin labeling. *J. Biol. Chem. 282*, 24970–24979.
8. Wirths, O., and Bayer, T. A. (2003) α-Synuclein, A$\beta$ and Alzheimer's disease. *Prog. Neuro-Psychopharmacol. Biol. Psychiatry 27*, 103–108.
9. Lucking, C. B., and Brice, A. (2000) α-Synuclein and Parkinson's disease. *Cell. Mol. Life Sci. 57*, 1894–1908.
10. Jao, C., Hegde, B., Chen, J., Haworth, I., and Langen, R. (2008) Structure of membrane-bound α-synuclein from site-directed spin labeling and computational refinement. *Proc. Natl. Acad. Sci. U.S.A. 105*, 19666.
11. Davidson, W. S., Jonas, A., Clayton, D. F., and George, J. M. (1998) Stabilization of α-synuclein secondary structure upon binding to synthetic membranes. *J. Biol. Chem. 273*, 9443–9449.
12. Zhou, W., Long, C., Reaney, S. H., Di Monte, D. A., Fink, A. L., and Uversky, V. N. (2010) Methionine oxidation stabilizes non-toxic oligomers of α-synuclein through strengthening the auto-inhibitory intramolecular long-range interactions. *Biochim. Biophys. Acta 1802*, 322–330.
13. Rybicki, B. A., Johnson, C. C., Uman, J., and Gorell, J. M. (1993) Parkinson's disease mortality and the industrial use of heavy metals in Michigan. *Mov. Disord. 8*, 87–92.
14. Singh, C., Ahmad, I., and Kumar, A. (2007) Pesticides and metals induced Parkinson's disease: Involvement of free radicals and oxidative stress. *Cell. Mol. Biol.* (*Paris, Fr., Print*) *53*, 19–28.
15. Barnham, K. J., and Bush, A. I. (2008) Metals in Alzheimer's and Parkinson's diseases. *Curr. Opin. Chem. Biol. 12*, 222–228.
16. Bisaglia, M., Tessari, I., Mammi, S., and Bubacco, L. (2009) Interaction Between α-Synuclein and Metal Ions, Still Looking for a Role in the Pathogenesis of Parkinson's Disease. *Neuromol. Med. 11*, 239–251.
17. Dexter, D. T., Carayon, A., Javoy-Agid, F., Agid, Y., Wells, F. R., Daniel, S. E., Lees, A. J., Jenner, P., and Marsden, C. D. (1991) Alterations in the levels of iron, ferritin and other trace metals in Parkinson's disease and other neurodegenerative diseases affecting the basal ganglia. *Brain 114* (Part 4), 1953–1975.
18. Pall, H., Blake, D., Gutteridge, J., Williams, A., Lunec, J., Hall, M., and Taylor, A. (1987) Raised cerebrospinal-fluid copper concentration in Parkinson's disease. *Lancet 330*, 238–241.
19. Bush, A. I. (2000) Metals and neuroscience. *Curr. Opin. Chem. Biol. 4*, 184–191.
20. Alimonti, A., Bocca, B., Pino, A., Ruggieri, F., Forte, G., and Sancesario, G. (2007) Elemental profile of cerebrospinal fluid in patients with Parkinson's disease. *J. Trace Elem. Med. Biol. 21*, 234–241.
21. Desai, V., and Kaler, S. G. (2008) Role of copper in human neurological disorders. *Am. J. Clin. Nutr. 88*, 855S–858S.
22. Uversky, V. N., Li, J., and Fink, A. L. (2001) Metal-triggered structural transformations, aggregation, and fibrillation of human α-synuclein. A possible molecular NK between Parkinson's disease and heavy metal exposure. *J. Biol. Chem. 276*, 44284–44296.
23. Millhauser, G. L. (2007) Copper and the prion protein: Methods, structures, function, and disease. *Annu. Rev. Phys. Chem. 58*, 299–320.
24. Sarell, C. J., Syme, C. D., Rigby, S. E., and Viles, J. H. (2009) Copper(II) binding to amyloid-$\beta$ fibrils of Alzheimer's disease reveals a picomolar affinity: Stoichiometry and coordination geometry are independent of A$\beta$ oligomeric form. *Biochemistry 48*, 4388–4402.
25. Millhauser, G. L. (2004) Copper Binding in the Prion Protein. *Acc. Chem. Res. 37*, 79–85.
26. Que, E. L., Domaille, D. W., and Chang, C. J. (2008) Metals in neurobiology: Probing their chemistry and biology with molecular imaging. *Chem. Rev. 108*, 1517–1549.
27. Chattopadhyay, M., Walter, E. D., Newell, D. J., Jackson, P. J., Aronoff-Spencer, E., Peisach, J., Gerfen, G. J., Bennett, B., Antholine, W. E., and Millhauser, G. L. (2005) The octarepeat domain of the prion protein binds Cu(II) with three distinct coordination modes at pH 7.4. *J. Am. Chem. Soc. 127*, 12647–12656.
28. Madsen, E., and Gitlin, J. D. (2007) Copper and iron disorders of the brain. *Annu. Rev. Neurosci. 30*, 317–337.
29. Lucas, H. R., Debeer, S., Hong, M. S., and Lee, J. C. (2010) Evidence for copper-dioxygen reactivity during α-synuclein fibril formation. *J. Am. Chem. Soc. 132*, 6636–6637.
30. Brown, D. R. (2007) Interactions between metals and α-synuclein: Function or artefact? *FEBS J. 274*, 3766–3774.
31. Kowalik-Jankowska, T., Rajewska, A., Jankowska, E., and Grzonka, Z. (2006) Copper(II) binding by fragments of α-synuclein containing M1-D2- and -H50-residues; a combined potentiometric and spectroscopic study. *Dalton Trans.*, 5068–5076.
32. Kowalik-Jankowska, T., Rajewska, A., Wisniewska, K., Grzonka, Z., and Jezierska, J. (2005) Coordination abilities of N-terminal fragments of α-synuclein towards copper(II) ions: A combined potentiometric and spectroscopic study. *J. Inorg. Biochem. 99*, 2282–2291.
33. Lee, J. C., Gray, H. B., and Winkler, J. R. (2008) Copper(II) binding to α-synuclein, the Parkinson's protein. *J. Am. Chem. Soc. 130*, 6898–6899.
34. Drew, S. C., Leong, S. L., Pham, C. L., Tew, D. J., Masters, C. L., Miles, L. A., Cappai, R., and Barnham, K. J. (2008) $Cu^{2+}$ binding modes of recombinant α-synuclein: Insights from EPR spectroscopy. *J. Am. Chem. Soc. 130*, 7766–7773.
35. Sung, Y. H., Rospigliosi, C., and Eliezer, D. (2006) NMR mapping of copper binding sites in α-synuclein. *Biochim. Biophys. Acta 1764*, 5–12.
36. Binolfi, A., Lamberto, G. R., Duran, R., Quintanar, L., Bertoncini, C. W., Souza, J. M., Cervenansky, C., Zweckstetter, M., Griesinger, C., and Fernandez, C. O. (2008) Site-specific interactions of Cu(II) with α- and $\beta$-synuclein: Bridging the molecular gap between metal binding and aggregation. *J. Am. Chem. Soc. 130*, 11801–11812.
37. Jackson, M. S., and Lee, J. C. (2009) Identification of the minimal copper(II)-binding α-synuclein sequence. *Inorg. Chem. 48*, 9303–9307.
38. Hong, L., and Simon, J. D. (2009) Binding of Cu(II) to human α-synucleins: Comparison of wild type and the point mutations associated with the familial Parkinson's disease. *J. Phys. Chem. B 113*, 9551–9561.
39. Kim, M., Elvin, C., Brownlee, A., and Lyons, R. (2007) High yield expression of recombinant pro-resilin: Lactose-induced fermentation in *E. coli* and facile purification. *Protein Expression Purif. 52*, 230–236.
40. Burns, C. S., Aronoff-Spencer, E., Dunham, C. M., Lario, P., Avdievich, N. I., Antholine, W. E., Olmstead, M. M., Vrielink, A., Gerfen, G. J., Peisach, J., Scott, W. G., and Millhauser, G. L. (2002) Molecular features of the copper binding sites in the octarepeat domain of the prion protein. *Biochemistry 41*, 3991–4001.
41. Uversky, V. N., Li, J., Souillac, P., Millett, I. S., Doniach, S., Jakes, R., Goedert, M., and Fink, A. L. (2002) Biophysical properties of the synucleins and their propensities to fibrillate: Inhibition of α-synuclein assembly by $\beta$- and $\gamma$-synucleins. *J. Biol. Chem. 277*, 11970–11978.
42. Sigel, H., and Martin, B. R. (1982) Coordinating Properties of the Amide Bond. Stability and Structure of Metal Ion Complexes of Peptides and Related Ligands. *Chem. Rev. 82*, 385–426.
43. Kallay, C., Varnagy, K., Micera, G., Sanna, D., and Sovago, I. (2005) Copper(II) complexes of oligopeptides containing aspartyl and

glutamyl residues. Potentiometric and spectroscopic studies. *J. Inorg. Biochem. 99*, 1514–1525.
44. Dikanov, S. A., and Tsvetkov, Y. D. (1992) Electron spin-echo envelope modulation (ESEEM) spectroscopy, CRC Press, Boca Raton, FL.
45. Mims, W. B., and Peisach, J. (1978) The nuclear modulation effect in electron spn echoes for complexes of Cu(II) and imidazole with $^{14}N$ and $^{15}N$. *J. Chem. Phys. 69*, 4921–4930.
46. Walter, E. D., Chattopadhyay, M., and Millhauser, G. L. (2006) The affinity of copper binding to the prion protein octarepeat domain: Evidence for negative cooperativity. *Biochemistry 45*, 13083–13092.
47. Wang, C., Liu, L., Zhang, L., Peng, Y., and Zhou, F. (2010) Redox reactions of the α-synuclein−$Cu^{2+}$ complex and their effects on neuronal cell viability. *Biochemistry 49*, 8134–8142.
48. Kanabrocki, E. L., Case, L. F., Miller, E. B., Kaplan, E., and Oester, Y. T. (1964) A Study of Human Cerebrospinal Fluid: Copper and Manganese. *J. Nucl. Med. 5*, 643–648.
49. Millhauser, G. L. (2007) Copper and the Prion Protein: Methods, Structures, Function, and Disease. *Annu. Rev. Phys. Chem. 58*, 299–320.
50. Chwiej, J., Adamek, D., Szczerbowska-Boruchowska, M., Krygowska-Wajs, A., Bohic, S., and Lankosz, M. (2008) Study of Cu chemical state inside single neurons from Parkinson's disease and control *substantia nigra* using the micro-XANES technique. *J. Trace Elem. Med. Biol. 22*, 183–188.
51. Chandra, S., Gallardo, G., Fernandez-Chacon, R., Schluter, O. M., and Sudhof, T. C. (2005) α-Synuclein cooperates with CSPα in preventing neurodegeneration. *Cell 123*, 383–396.
52. Bonini, N. M., and Giasson, B. I. (2005) Snaring the function of α-synuclein. *Cell 123*, 359–361.
53. Burre, J., Sharma, M., Tsetsenis, T., Buchman, V., Etherton, M. R., and Sudhof, T. C. (2010) α-Synuclein promotes SNARE-complex assembly in vivo and in vitro. *Science 329*, 1663–1667.